

Synthesis, geometrical and electronic structure of iron mononitrosyl complexes with bis(*S*-alkylisothiosemicarbazones) of β -dicarbonyl compounds

N. V. Gerbeleu, V. B. Arion*, Yu. A. Simonov, V. E. Zavodnik, S. S. Stavrov**, K. I. Turta, D. I. Gradinaru, M. S. Birca

Institute of Chemistry, Institute of Applied Physics, Moldova Academy of Sciences, Academy Street 3, 277028 Kishinev (Moldova)

A. A. Pasynskii and O. Ellert

Institute of General and Inorganic Chemistry, Russia Academy of Sciences, Leninskii Prospect 31, 117907 Moscow (Russia)

(Received April 16, 1992; revised July 15, 1992)

Abstract

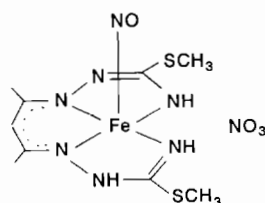
Complex $[\text{Fe}(\text{HL})\text{NO}]\text{NO}_3$ (**1**), where $\text{H}_3\text{L}=2,4$ -pentanedione bis(*S*-methylisothiosemicarbazone), has been synthesized by template reaction of *S*-methylisothiosemicarbazidehydrogen-nitrate, sodium acetylacetonate monohydrate and $\text{Fe}(\text{NO}_3)_3 \cdot 9\text{H}_2\text{O}$ in ethanol, while $[\text{Fe}(\text{R}_2\text{Q})\text{NO}]$ (**2**), where $\text{R}=\text{CH}_3$ (**2a**), C_2H_5 (**2b**), $n\text{-C}_3\text{H}_7$ (**2c**), $n\text{-C}_4\text{H}_9$ (**2d**), has been obtained by the interaction of $\text{Fe}(\text{NO}_3)_3 \cdot 9\text{H}_2\text{O}$ with nitromalondialdehyde bis(*S*-methylisothiosemicarbazone) ($\text{R}_3\text{H}_3\text{Q}$) in the presence of nitric oxide in ethanol. The crystal structures of **1** and **2c** have been determined by X-ray diffraction methods. Crystal **1** belongs to the monoclinic system, space group $P2_1/n$; $a=7.660(1)$, $b=21.092(2)$, $c=10.385(2)$ Å, $\gamma=96.15(2)^\circ$, $\rho_{\text{calc}}=1.367$ g cm $^{-3}$, $Z=4$, molecular formula $\text{C}_9\text{H}_{16}\text{FeN}_8\text{O}_3\text{S}_2$. Crystal **2c** is triclinic, space group $P1$; $a=8.108(2)$, $b=9.489(2)$, $c=12.872(3)$ Å, $\alpha=103.51(2)$, $\beta=106.02(2)$, $\gamma=75.09(2)^\circ$, $\rho_{\text{calc}}=1.578$ g cm $^{-3}$, $Z=2$, molecular formula $\text{C}_{11}\text{H}_{18}\text{FeN}_8\text{O}_3\text{S}_2$. The structures **1** (**2c**) were solved by direct methods. Least-squares refinement using 1829 (1794) unique reflections with $I \geq 3\sigma(I)$ has led to the final R of 0.026 (0.034) for **1** (**2c**). The cation $[\text{Fe}(\text{HL})\text{NO}]^+$ and complex **2c** have a square-pyramidal structure with the corresponding quadridentate ligand (HL^{2-} and $\text{C}_3\text{H}_7\text{Q}^{3-}$) around the central ion in the basal plane (deviation from the pyramid base plane 0.477 (**1**) and 0.473 (**2c**) Å) and the NO in the apical position. The FeNO group is approximately linear (the FeNO angle is equal to 172.7 (175.5°)). The data of the ^1H NMR, IR, Mössbauer and electronic absorption spectra indicate that **2a–2d** have a similarly structured coordination polyhedron. On the basis of X-ray analysis, IR, Mössbauer spectra and calculations of the electronic structures, it was concluded that the FeNO group is a highly covalent entity.

Introduction

Complexes of diatomic molecules with macrocyclic coordination compounds and their relationship to heme-protein complexes are of current interest [1–3]. In particular, studies of iron mononitrosyl compounds [4–7] may provide an insight into the nature of the heme-protein–nitric oxide complexes and the reductive nitrosylation reaction.

Chelates of metals with quadridentate ligands based on thioalkylated isothiosemicarbazides resemble macrocyclic complexes in a variety of properties [8].

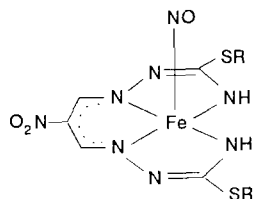
In this paper we report data on the synthesis, geometrical and electronic structure of iron mononitrosyl complexes $[\text{Fe}(\text{HL})\text{NO}]\text{NO}_3$ (**1**), where $\text{H}_3\text{L}=2,4$ -pentanedione bis(*S*-methylisothiosemicarbazone), and $[\text{Fe}(\text{R}_2\text{Q})\text{NO}]$ (**2**) ($\text{H}_3\text{R}_2\text{Q}=\text{nitromalondialdehyde bis}(\text{S}\text{-alkylisothiosemicarbazone})$), where $\text{R}=\text{CH}_3$ (**2a**), C_2H_5 (**2b**), $n\text{-C}_3\text{H}_7$ (**2c**), $n\text{-C}_4\text{H}_9$ (**2d**).



$[\text{Fe}(\text{HL})\text{NO}]\text{NO}_3$ (**1**)

*Author to whom correspondence should be addressed.

**Present address: Sackler Institute of Molecular Medicine, Sackler Faculty of Medicine, Tel Aviv University, P.O.B. 39040, Ramat-Aviv, Tel Aviv 69978, Israel.



[Fe(R₂Q)NO] (2), R = CH₃ (2a), C₂H₅ (2b), n-C₃H₇ (2c), n-C₄H₉ (2d)

Experimental

All chemicals used were analytical reagent grade. *S*-Methylisothiosemicarbazidehydrogen-nitrate, sodium acetylacetonate monohydrate, the sodium salt of nitromalondialdehyde monohydrate and nitromalondialdehyde bis (*S*-methylisothiosemicarbazone) were prepared according to known procedures, described in refs. 9–12, respectively.

Caution: *S*-methylisothiosemicarbazidehydrogen-nitrate is highly explosive! Do not heat any such nitrate salts!

Synthesis of [Fe(HL)NO]NO₃ (1)

To a solution of 1.68 g (10 mmol) of *S*-methylisothiosemicarbazidehydrogen-nitrate in 10 cm³ of ethanol were added 0.70 g (5 mmol) of sodium acetylacetonate monohydrate in 10 cm³ of ethanol and 2.00 g (5 mmol) of Fe(NO₃)₃·9H₂O in 10 cm³ of ethanol. After 8–10 days, the crystals were separated by filtration and washed with ethanol, and water, again with ethanol, and finally with ether. Yield 0.11 g (5%) of black crystalline product.

Synthesis of [Fe(R₂Q)NO], where R = CH₃ (2a)

To a suspension of 0.72 g (2.5 mmol) of nitromalondialdehyde bis(*S*-methylisothiosemicarbazone) (H₃(CH₃)₂Q) in 10 cm³ of ethanol was added 1.00 g of Fe(NO₃)₃·9H₂O in 10 cm³ of ethanol and nitric oxide was passed through the resulting solution until precipitation began. The black crystal were filtered off and washed with ethanol and ether. Yield 0.26 g (28%).

The complexes **2b**, **2c** and **2d** were prepared in an analogous way with the yields 0.22 (22%), 0.19 (18%) and 0.21 (19%) g, respectively.

Single crystals of **1** suitable for the X-ray analysis were selected from the synthesized product.

Single crystals of **2c** were grown from a chloroform–ethanolic solution at room temperature in a thermostat.

Characterization of complexes

[Fe(HL)NO]NO₃ (**1**). *Anal.* Calc. for C₉H₁₆-FeN₈O₄S₂ (FW=420.25): C, 25.72; H, 3.84; N, 26.66. Found: C, 26.14; H, 3.66; N, 26.48%. Electronic spectrum

(CHCl₃) λ_{max} (nm) (log ε): 299 (4.20), 355 (4.08), 667 (3.31). IR (Nujol mull): ν(NO) 1800 cm⁻¹.

[Fe(CH₃)₂Q(NO)] (**2a**). *Anal.* Calc. for C₇H₁₀-FeN₈O₃S₂ (FW=374.18): C, 22.48; H, 2.89; N, 29.95. Found: C, 22.68; H, 3.22; N, 30.39%. Electronic spectrum (CHCl₃) λ_{max} (nm) (log ε): 318 (4.50), 365sh (4.18), 467 (3.38), 588 (3.28), 737 (3.57). IR (Nujol mull): ν(NO) 1802 cm⁻¹. ¹H NMR {(CD₃)₂SO}: δ 2.77, s, 6H, SCH₃; 9.39, s, 2H, CH; 9.74, b, 2H, NH.

[Fe(C₂H₅)₂Q(NO)] (**2b**). *Anal.* Calc. for C₉H₁₄-FeN₈O₃S₂ (FW=402.24): C, 26.87; H, 3.51; N, 27.87. Found: C, 26.56; H, 3.38; N, 28.28%. Electronic spectrum (CHCl₃) λ_{max} (nm) (log ε): 317 (4.35), 357sh (4.21), 472 (3.38), 598 (3.30), 740 (3.55). IR (Nujol mull): ν(NO) 1804 cm⁻¹. ¹H NMR (CDCl₃): δ 1.44, t, 6H, CH₃; 3.14–3.41, m, 4H, CH₂; 7.44, b, 2H, NH; 9.54, s, 2H, CH.

[Fe(n-C₃H₇)₂Q(NO)] (**2c**). *Anal.* Calc. for C₁₁H₁₈-FeN₈O₃S₂ (FW=430.29): C, 30.71; H, 4.22; N, 26.04. Found: C, 30.80; H, 3.79; N, 25.79]. Electronic spectrum (CHCl₃) λ_{max} (nm) (log ε): 315 (4.37), 363sh (4.23), 459 (3.41), 601 (3.31), 740 (3.58). IR (Nujol mull): ν(NO) 1808 cm⁻¹. ¹H NMR (CDCl₃): δ 1.07, t, 6H, CH₃; 1.62–1.94, m, 4H, CH₂; 3.16–3.35, m, 4H, CH₂; 7.50, b, 2H, NH; 9.54, s, 2H, CH.

[Fe(n-C₄H₉)₂Q(NO)] (**2d**). *Anal.* Calc. for C₁₃H₂₂FeN₈O₃S₂ (FW=458.34): C, 34.07; H, 4.84; N, 24.55. Found: C, 33.76; H, 4.58; N, 25.16%. Electronic spectrum (CHCl₃) λ_{max} (nm) (log ε): 318 (4.35), 362sh (4.22), 459 (3.42), 609 (3.20), 741 (3.54). IR (Nujol mull): ν(NO) 1796 cm⁻¹. ¹H NMR (CDCl₃): δ 0.87–1.04, m, 6H, CH₃; 1.35–1.99, m, 4H, CH₂; 3.18–3.35, m, 4H, CH₂; 7.53, b, 2H, NH, 9.53, s, 2H, CH.

The C, H, N contents were determined by standard micro-methods. IR spectra were recorded on a UR-20 spectrometer. Electronic spectra (C = 10⁻⁴ mol dm⁻³) were obtained using a Specord M40 spectrophotometer. ¹H NMR spectra were recorded at 80 MHz on a Bruker PW 80. Spectra were measured from the solutions of the complexes in (CD₃)₂SO, and CDCl₃ with tetramethylsilane as internal reference. Magnetic susceptibilities were measured by the Faraday method for **1** and on a Gouy apparatus for **2a–2d**. ⁵⁷Fe Mössbauer measurements were carried out with powder samples of about 100 mg in polyethylene containers of 19 mm diameter at 300 and 80 K; spectra were recorded with a spectrometer consisting of a constant acceleration electronic drive and a Nuclear multichannel analyzer ICA-70 (Hungary) operating in the multiscaling mode. The γ-source used consisted of 15 mCi of ⁵⁷Co in chromium at room temperature, the calibration being effected with an iron-foil absorber. All velocity scales and isomer shifts are referred to the sodium nitroprusside standard at 300 K. For conversion to the iron scale, -0.257 mm s⁻¹ has to be added.

Collection and reduction of X-ray data

A suitable black plate-like monocrystal of **1** (**2c**), dimensions $0.22 \times 0.20 \times 0.11$ ($0.15 \times 0.20 \times 0.15$) mm, was put in an Enraf-Nonius CAD-4 (Nicolet P3) diffractometer to collect reflection data. Elementary cell parameters were measured and refined from results of 15 strong high-angle reflections $h00$, $0k0$ and $00l$ type. The intensities were measured at 293 (295) K using the $\theta/2\theta$ scanning technique. The method of profile analysis of peaks for the monochromated Mo $K\alpha$ radiation ($\lambda = 0.71069 \text{ \AA}$) was employed. Three standard reflections were measured after collecting 100 reflections. Corrections were applied for Lorentz and polarization factors. An empirical absorption was applied taking into account the form of the crystal according to SHELXS-86 [13]. To determine and refine the crystal structures, 1829 (1794) reflections satisfying $I \geq 3\sigma(I)$ were used; the dependent reflections were averaged. The structures were solved by the direct method using the SHELXS-86 programme [13] and atomic factors from ref. 14 including anomalous dispersion (f , f' and f''). The structures were refined by full-matrix least-squares techniques with anisotropic approximations for C, N, O, S, Fe and isotropic for H. The H atoms were obtained from differential Fourier synthesis. The refinement was carried out using the weighting schemes $w = 1/[\sigma(F) + 0.000022F^2]$ and $w = 1/[\sigma(F) + 0.004981F^2]$ for **1** and **2c**, respectively. The crystallographic data, atom coordinates and equivalent isotropic temperature factors, interatomic distances and angles are given in Tables 1–5, respectively.

TABLE 1. Crystallographic data for complexes **1** and **2c**

	1	2c
Chemical formula	$C_9H_{16}FeN_8O_4S_2$	$C_{11}H_{18}FeN_8O_3S_2$
Formula weight	420.25	430.29
System	monoclinic	triclinic
a (Å)	7.660(1)	8.108(2)
b (Å)	21.092(2)	9.489(2)
c (Å)	10.385(2)	12.872(3)
α (°)		103.51(2)
β (°)		106.02(2)
γ (°)	96.15(2)	75.09(2)
V (Å ³)	1668.2(8)	905.6(7)
Z	4	2
Space group	$P2_1/n$	$P\bar{1}$
T (°C)	20	22
λ (Å)	0.71069	0.71069
ρ_{calc}	1.367	1.578
μ (cm ⁻¹)	11.44	10.80
Scan speed (°/min)	3–12	3–12
2θ Range (°)	$3 < 2\theta < 45$	$3 < 2\theta < 45$
R^a	0.026	0.034
R_w^b	0.028	0.036

$$^a R = \sum |F_o| - |F_c| / \sum |F_o| \quad ^b R_w = [\sum w(|F_o| - |F_c|)^2 / \sum w |F_o|^2]^{1/2}$$

TABLE 2. Atom coordinates ($\times 10^4$) and equivalent isotropic temperature factors ($\text{\AA}^2 \times 10^3$) with their e.s.d.s for complex **1**

Atom	x	y	z	U_{eq}^a
Fe	2166(1)	6022(1)	5760(1)	30(1)
S1	-0752(1)	7626(1)	7054(1)	45(1)
S2	2937(1)	4086(1)	7032(1)	43(1)
N1	0784(3)	6512(1)	6870(3)	36(1)
N2	0388(3)	7040(1)	5053(3)	37(1)
N3	1204(3)	6549(1)	4505(2)	32(1)
N4	2284(3)	5363(1)	4547(2)	32(1)
N5	2558(3)	4779(1)	5007(2)	37(1)
N6	2016(3)	5303(1)	6857(3)	37(1)
N7	4208(3)	6336(1)	5961(2)	37(1)
N8	3717(4)	6351(1)	9370(2)	49(1)
O1	5694(3)	6507(1)	6015(3)	64(1)
O2	5118(4)	6714(1)	9260(3)	67(1)
O3	3782(4)	5774(1)	9376(3)	84(1)
O4	2344(4)	6600(1)	9486(2)	72(1)
C1	0216(3)	7003(1)	6335(3)	32(1)
C2	1388(3)	6535(1)	3236(3)	32(1)
C3	2024(4)	5995(1)	2673(3)	35(1)
C4	2363(3)	5434(1)	3242(3)	34(1)
C5	2438(3)	4787(1)	6286(3)	32(1)
C6	0873(5)	7061(2)	2416(4)	41(1)
C7	2785(5)	4880(2)	2441(4)	47(1)
C8	-0981(7)	7348(2)	8678(4)	64(2)
C9	2515(6)	4241(2)	8697(4)	56(1)

^aEquivalent isotropic U_{eq} defined as one third of the trace of the orthogonalized U_{ij} tensor, $U_{\text{eq}} = 1/3 \text{ trace } \bar{U}$.

Results and discussion

The complex transformations, which take place in the coordination sphere of Fe^{3+} as a result of the interaction of sodium acetylacetonate and *S*-methylisothiosemicarbazidehydrogen-nitrate, lead to the formation of 2,4-pentanedione bis(*S*-methylisothiosemicarbazone) (H_3L) and nitric oxide, which are isolated as $[\text{Fe}(\text{HL})\text{NO}]\text{NO}_3$ (**1**). The reaction of $\text{Fe}(\text{NO}_3)_3 \cdot 9\text{H}_2\text{O}$ with the corresponding nitromalon-dialdehyde bis(*S*-alkylisothiosemicarbazone) in the presence of nitric oxide gives rise to the production of **2**. All the substances are black crystals which are well soluble in DMSO and acetone, less soluble in methanol and ethanol, and insoluble in hexane and water. The solubility in chloroform is the lowest for ionic complex **1** and increases in the sequence $\mathbf{2a} < \mathbf{2d}$ simultaneously with the bulk of alkyl substituent. The thermal stability of **1** is lower than for **2**. Thus the complex $[\text{Fe}(\text{HL})\text{NO}]\text{NO}_3$ is stable up to ~ 110 °C, whereas **2c** starts to decompose at ~ 230 °C.

Crystallographic studies

In Fig. 1 the structure of the cation $[\text{Fe}(\text{HL})\text{NO}]^+$ is presented. The square-pyramidal configuration is formed by the quadridentate ligand in the base (distances Fe–N1, Fe–N3, Fe–N4, Fe–N6 are 1.937(3),

TABLE 3. Atom coordinates ($\times 10^4$) and equivalent isotropic temperature factors ($\text{\AA}^2 \times 10^3$) with their e.s.d.s for complex 2c

Atom	x	y	z	U_{eq}^a
Fe	3138(1)	6987(1)	6061(1)	37(1)
S1	7677(2)	8030(1)	8723(1)	61(1)
S2	0300(2)	8379(1)	2914(1)	71(1)
O1	0490(5)	7753(5)	7204(3)	83(2)
O2	4532(5)	1237(3)	6354(3)	73(1)
O3	2488(5)	1338(3)	4883(3)	78(2)
N1	4932(6)	8029(4)	6889(3)	46(1)
N2	6046(5)	5930(3)	7665(3)	45(1)
N3	4770(4)	5495(3)	6801(2)	38(1)
N4	2306(4)	5555(3)	4859(2)	38(1)
N5	1287(5)	6036(3)	3920(2)	46(1)
N6	2341(6)	8089(4)	4909(3)	49(2)
N7	1611(5)	7487(4)	6737(3)	47(1)
N8	3518(5)	1909(3)	5652(3)	52(2)
C1	6060(6)	7345(4)	7655(3)	43(2)
C2	4668(6)	4070(4)	6635(3)	41(2)
C3	3516(6)	3476(3)	5745(3)	41(2)
C4	2418(6)	4130(4)	4874(3)	44(2)
C5	1410(6)	7449(4)	4016(3)	43(2)
C6	7496(9)	9864(6)	8500(4)	77(3)
C7	6420(15)	11014(8)	9050(6)	116(5)
C8	6933(16)	11263(10)	10326(6)	95(4)
C9	-0247(9)	6854(6)	1784(4)	72(3)
C10	-1854(10)	6379(8)	1788(5)	86(3)
C11	-2317(16)	5234(10)	0755(7)	109(4)

^aEquivalent isotropic U_{eq} defined as one third of the trace of the orthogonalized U_{ij} tensor, $U_{eq} = 1/3$ trace \hat{U} .

1.911(2), 1.886(3), 1.888(3) Å, respectively) and NO in the apical position (Fe–N7 1.645(2) Å). The four nitrogen atoms, N1, N3, N4, N6, are coplanar, the metal ion being raised from the plane to the NO site by 0.477 Å.

The ligand HL²⁻ appears as a result of deprotonation of the acetylacetonate moiety and of one isothiosemicarbazide fragment. The non-equivalence of the isothiosemicarbazide residues was proved by direct proton location at N2 and its absence at N5. It should be noted that *S*-methylisothiosemicarbazide fragments are the same in Ni(H₂L)I described previously [15].

In the coordination of HL²⁻ with the iron atom, three metallo rings are formed: one six-membered FeN₂C₃ and two five-membered FeN₃C. All of them possess an envelope conformation with the displacement of the Fe atom from the six-membered ring plane by -0.474 Å, and from the planes of the two five-membered rings by -0.303 and -0.326 Å. The chelate angle N3–Fe–N4 is equal to 91.4°, that is somewhat greater than in five-membered ones (N1–Fe–N3 80.2°, N4–Fe–N6 79.4°). Another difference between the five-membered rings is the bond distribution in them. Thus the geometrical parameters in the metallo ring formed by the protonated isothiosemicarbazide fragment (N1–C1 = 1.291, C1–N2 = 1.339, N2–N3 = 1.389 Å) are

TABLE 4. Bond lengths (Å) for complexes 1 and 2c

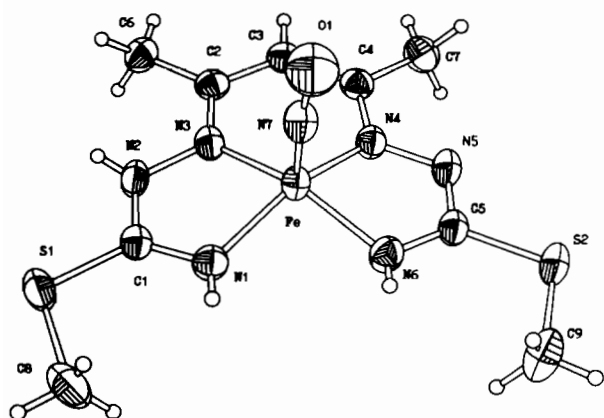
Complex 1			
Fe–N1	1.937(3)	Fe–N6	1.888(3)
Fe–N3	1.911(2)	Fe–N4	1.886(2)
Fe–N7	1.645(2)	N7–O1	1.158(3)
N1–C1	1.291(4)	N6–C5	1.313(4)
C1–S1	1.743(3)	C5–S2	1.748(3)
C8–S1	1.788(4)	C9–S2	1.795(4)
C1–N2	1.339(4)	C5–N5	1.331(4)
N2–N3	1.389(3)	N5–N4	1.359(3)
N3–C2	1.326(4)	N4–C4	1.364(4)
C2–C3	1.414(4)	C4–C3	1.372(4)
C2–C6	1.485(5)	C4–C7	1.496(5)
N8–O2	1.258(4)	N8–O3	1.225(4)
N8–O4	1.227(4)		
Complex 2c			
Fe–N1	1.903(4)	Fe–N6	1.887(4)
Fe–N3	1.906(3)	Fe–N4	1.900(3)
Fe–N7	1.618(4)	N7–O1	1.167(6)
N1–C1	1.314(5)	N6–C5	1.300(5)
C1–S1	1.748(4)	C5–S2	1.754(4)
C1–N2	1.349(5)	C5–N5	1.344(5)
N2–N3	1.360(4)	N5–N4	1.365(4)
N3–C2	1.339(5)	N4–C4	1.336(5)
C2–C3	1.372(5)	C4–C3	1.387(5)
C3–N8	1.463(5)		
N8–O2	1.220(5)	N8–O3	1.224(5)
C6–S1	1.792(6)	C9–S2	1.843(5)
C6–C7	1.39(1)	C9–C10	1.49(1)
C7–C8	1.56(1)	C10–C11	1.53(1)

similar to the ones for Ni(H₂L)I (N1–C1 = 1.297, C1–N2 = 1.337, N2–N3 = 1.403 Å) [15]. In the deprotonated five-membered FeN₃C ring the bond N5–N4 = 1.359 Å has been considerably shortened, the bond C5–N5 = 1.331 Å is not significantly altered, whereas the bond N6–C5 = 1.313 Å is somewhat elongated compared to the respective bonds of the protonated ring. The deprotonated FeN₃C metallo ring is smaller in perimeter than the protonated one. The non-equivalence of the FeN₃C rings affects the distribution of bonds in the six-membered FeN₂C₃ ring. Thus N3–C2 (1.326 Å) is significantly shorter than N4–C4 (1.364 Å), whereas C2–C3 (1.414 Å) is longer than C3–C4 (1.372 Å). It should be noted that the respective distances are almost the same as in Ni(H₂L)I [15] (N3–C2 = 1.324, N4–C4 = 1.326; C2–C3 = 1.399, C3–C4 = 1.394 Å). The X-ray data have shown the FeNO group to be almost linear (\angle FeNO = 172.7°).

The methyl groups linked to the sulfur atoms (S1 and S2) in [Fe(HL)NO]NO₃ (as in the case of Ni(H₂L)I) are oriented towards N1 and N6, respectively. The sulfur atoms S1 and S2 deviate from the plane of the corresponding FeN₃C moiety by -0.040 and -0.129 Å, respectively. In the thioether fragments the C–S distances are as follows: C1–S1 (C5–S2) = 1.743 (1.748) Å; C8–S1 (C9–S2) = 1.788 (1.795) Å.

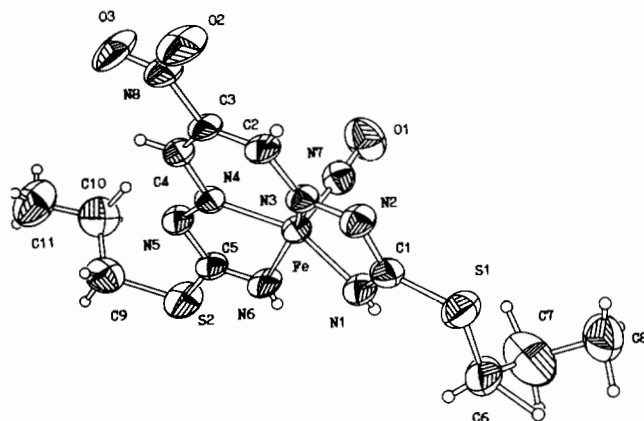
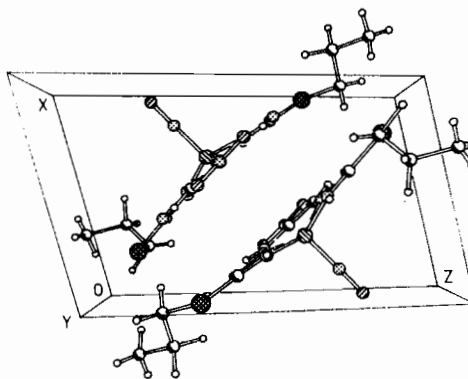
TABLE 5. Bond angles (°) for complexes **1** and **2c**

Complex 1			
N1-Fe-N3	80.2(1)	N4-Fe-N6	79.4(1)
N3-Fe-N4	91.4(1)	N1-Fe-N6	94.5(1)
N1-Fe-N4	149.7(1)	N3-Fe-N6	152.0(1)
N1-Fe-N7	105.1(1)	N6-Fe-N7	102.7(1)
N3-Fe-N7	105.2(1)	N4-Fe-N7	105.2(1)
Fe-N1-C1	115.0(2)	Fe-N6-C5	113.2(2)
S1-C1-N1	128.8(2)	S2-C5-N6	126.8(2)
N1-C1-N2	115.8(3)	N6-C5-N5	119.0(3)
S1-C1-N2	115.4(2)	S2-C5-N5	114.2(2)
C1-N2-N3	114.4(2)	C5-N5-N4	108.8(3)
Fe-N3-N2	112.7(2)	Fe-N4-N5	117.2(2)
N2-N3-C2	118.7(2)	N5-N4-C4	116.1(2)
Fe-N3-C2	128.1(2)	Fe-N4-C4	126.1(2)
N3-C2-C6	121.1(3)	N4-C4-C7	118.5(3)
N3-C2-C3	118.3(3)	N4-C4-C3	120.8(3)
C3-C2-C6	120.5(3)	C3-C4-C7	120.7(3)
C2-C3-C4	129.1(3)		
Complex 2c			
N1-Fe-N3	78.7(1)	N4-Fe-N6	78.6(1)
N3-Fe-N4	92.0(1)	N1-Fe-N6	96.3(2)
N1-Fe-N4	150.3(2)	N3-Fe-N6	151.8(2)
N1-Fe-N7	106.0(2)	N6-Fe-N7	105.3(2)
N3-Fe-N7	102.7(2)	N4-Fe-N7	103.6(1)
Fe-N1-C1	113.5(3)	Fe-N6-C5	114.3(3)
S1-C1-N1	128.2(3)	S2-C5-N6	121.7(3)
C1-S1-C6	103.9(2)	C5-S2-C9	102.6(2)
N1-C1-N2	119.4(4)	N6-C5-N5	120.0(4)
S1-C1-N2	112.3(3)	S2-C5-N5	118.3(3)
C1-N2-N3	107.9(3)	C5-N5-N4	106.9(3)
Fe-N3-N2	117.8(2)	Fe-N4-N5	118.0(2)
N2-N3-C2	115.7(3)	N5-N4-C4	114.9(3)
Fe-N3-C2	126.0(2)	Fe-N4-C4	126.5(2)
N3-C2-C3	121.1(3)	N4-C4-C3	120.6(3)
C2-C3-C4	128.8(4)		
C2-C3-N8	116.2(3)	C4-C3-N8	114.8(3)
C3-N8-O2	118.4(3)	C3-N8-O3	118.6(3)
O2-N8-O3	123.1(4)		
S1-C6-C7	117.1(6)	Se-C9-C10	113.3(4)
C6-C7-C8	116.8(7)	C9-C10-C11	109.6(7)

Fig. 1. ORTEP view of the complex cation $[\text{Fe}(\text{HL})\text{NO}]^+$ structure showing the atom-numbering scheme.

The NO_3 group is perfectly planar with the N–O distance ranging from 1.224 to 1.257 Å. It has a bridging function and links complex cations giving chains formed along the z axis. Thus, the basal cation and the basal anion NO_3^- are linked together by an $\text{N1-H100}\dots\text{O4}=2.966$ Å hydrogen bond. At the same time $[\text{Fe}(\text{HL})\text{NO}]^+$ is linked with another anion NO_3^- , formed from the basal one by symmetry transformation $\frac{1}{2}-x, 1\frac{1}{2}-y, \frac{1}{2}+z$, via an $\text{N2-H200}\dots\text{O2}=2.820$ Å hydrogen bond ($\text{H200}\dots\text{O2}=2.10$ Å). There are only van der Waals interactions between chains.

The molecular structure of **2c** is shown in Fig. 2 and the unit cell packing diagram in Fig. 3. As in the case of **1** the iron coordination polyhedron of **2c** is a square pyramid. In the basal plane to the central ion three times deprotonated nitromalondialdehyde bis(*S*-propylisothiosemicarbazone) ($(n\text{-C}_3\text{H}_7)_2\text{Q}^{3-}$) is coordinated by N1, N3, N4 and N6 atoms. The interatomic distances Fe–N1, Fe–N3, Fe–N4 and Fe–N6 are equal to 1.903(4), 1.906(3), 1.887(4) and 1.900(3) Å, respectively. The NO group is in the apical position of the square pyramid (Fe–N7 = 1.618(4) Å, N7–O1 = 1.167(6) Å, Fe–N7–O1 = 175.5(4)°). The displacement of the iron atom from the basal plane of the pyramid is 0.473 Å toward

Fig. 2. ORTEP view of the complex **2c** structure showing the atom-numbering scheme.Fig. 3. The unit cell packing diagram for **2c**.

NO. As in the case of **1** all three metallo rings formed in the coordination of the quadridentate ligand with the iron atom possess an envelope conformation. The displacement of the Fe atom from the six-membered ring plane is -0.427 \AA , and from the planes of the two five-membered rings it is -0.315 and -0.356 \AA . The chelate angle N3–Fe–N4 (92.0°) is close to that for **1**. The angles N1–Fe–N3 and N4–Fe–N6 are practically the same (78.7 and 78.6°) in the two five-membered FeN₃C rings. The distribution of bonds in these rings also indicates their geometrical similarity. The interatomic distances N1–C1 (N6–C5), C1–N2 (C5–N5), N2–N3 (N5–N4) in the isothiosemicarbazide moieties are equal to 1.314 (1.300), 1.349 (1.344), 1.360 (1.365) \AA , respectively.

It should be noted that the six-membered chelate ring is essentially planar, with equivalent C–C and C–N bonds (the bond lengths N3–C2, C2–C3, C3–C4 and C4–N4 are equal to 1.339, 1.372, 1.387 and 1.336 \AA , respectively) indicating extensive delocalization over the chelate ring. The central C2–C3–C4 bond angle for this compound is about 129° .

The plane of the NO₂ group forms an angle of 3.2° with the organic portion of the six-membered metallo ring.

In the crystal structure the NH groups act as donors in the hydrogen bonds of the N–H...O type: N1...O2 ($x, 1+y, z$) = 3.193 \AA and N6...O3 ($x, 1+y, z$) = 3.124 \AA join the complexes linked by the translation motion in chains via double bridges. The parameters of the H bonds are: N1–H = 0.63, H...O2 = 2.59 \AA , the angle at H atom is 163° , and N6–H = 0.65, H...O3 = 2.54 \AA , the angle at H is equal to 171° .

The Mössbauer spectra (Table 6, Figs. 4 and 5) of diamagnetic (according to the ¹H NMR data and magnetochemistry) complexes **1** and **2a–3d** at 300 and 80 K are of the doublet form with approximately equal intensities and equal linewidths. The isomer shifts (relative to sodium nitroprusside) are 0.24 and 0.15–0.18

TABLE 6. Mössbauer spectra parameters^a

Complex	<i>T</i> (K)	δ (mm s ⁻¹)	ΔE_q (mm s ⁻¹)	Γ_1^b (mm s ⁻¹)	Γ_r^c (mm s ⁻¹)
1	300	0.24	1.18	0.28	0.30
	80	0.30	1.18	0.36	0.39
2a	300	0.16	1.64	0.28	0.25
	80	0.23	1.67	0.32	0.29
2b	300	0.17	1.80	0.29	0.37
	80	0.20	1.76	0.28	0.30
2c	300	0.18	1.61	0.26	0.33
	80	0.23	1.63	0.30	0.33
2d	300	0.15	1.66	0.28	0.31
	80	0.21	1.72	0.29	0.31

^aThe accuracy of Mössbauer spectra parameters is $\pm 0.04 \text{ mm s}^{-1}$. ^bLeft linewidth. ^cRight linewidth.

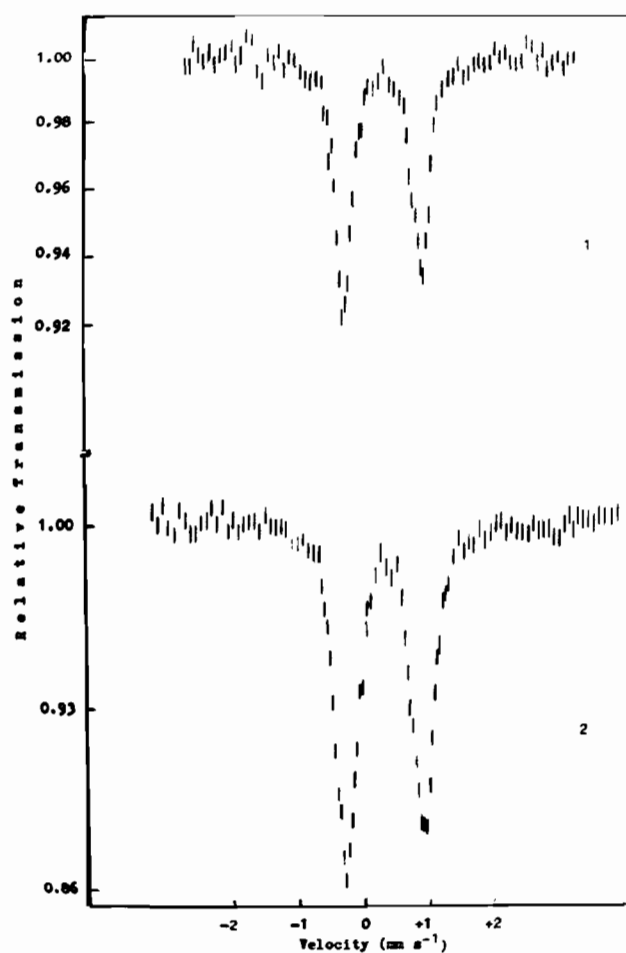


Fig. 4. Mössbauer spectra of [Fe(HL)NO]NO₃ recorded at 300 (1) and 80 (2) K. The number of counts per velocity point is approximately equal to 110500 (300 K) and 95340 (80 K).

mm s⁻¹ at 300 K for **1** and **2a–2d**, respectively. An increase in δ (at 80 K, see Table 6), that may be attributable, at least in part, to a second order Doppler shift arising from lattice effects, is observed. The ΔE_Q values are almost independent of temperature (Table 6), however they are considerably different for **1** and **2a–2d**. The Mössbauer spectra parameters indicate a high degree of covalency in the metal–ligand bonds. Strong support for this conclusion comes from a comparative analysis of the Mössbauer spectra of **1** and **2** with those of Na₂[Fe(CN)₅NO] [16].

The results of ¹H NMR and electronic spectra treatment of **2a–2d** are listed in 'Experimental'. The ¹H NMR spectra of **2b–2d** in CDCl₃ show one aldimine proton resonance at δ 9.53–9.54 ppm and one NH resonance (broad singlet at δ 7.44–7.53 ppm). The remaining resonances are assigned to thioalkyl hydrogens. The expected downfield shift of the NH proton resonance for **2a** (δ 9.74 ppm) in (CD₃)₂SO is observed, which is probably a consequence of hydrogen bonding between NH groups and (CD₃)₂SO molecules. The

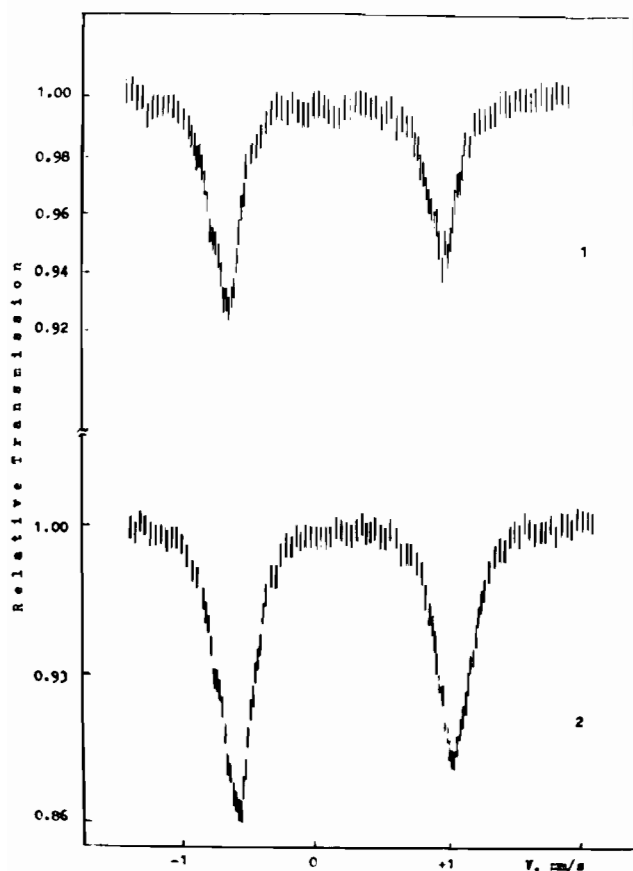
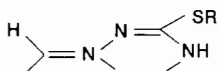


Fig. 5. Mössbauer spectra of **2a** recorded at 300 (1) and 80 (2) K. The number of counts per velocity point is approximately equal to 214720 (300 K) and 161240 (80 K).

number of resonance signals in the ^1H NMR spectra of **2a–2d** (see above) indicates the close similarity of the two moieties



in the molecules. At the same time the resonances of the thioalkyl hydrogens in **2b–2d** point to a small non-equivalence of SR protons, caused, probably, by a different orientation of the substituents of the sulfur atoms.

The ^1H NMR, Mössbauer, electronic and IR spectra show that the coordination on polyhedron of all **2 (a–d)** complexes has the same structure.

The self-consistent charge molecular orbital (SCC-MO) calculations of **1 (2c)** within the framework of the Mulliken–Wolfsberg–Helmhorz variant [17] of the extended Hückel method were performed for the elucidation of their structural and spectroscopic characteristics.

In Fig. 6 the diagram of the highest occupied (HOMO) and the lowest unoccupied (LUMO) MOs of **1 (2c)** are shown, and, if possible, their atomic composition

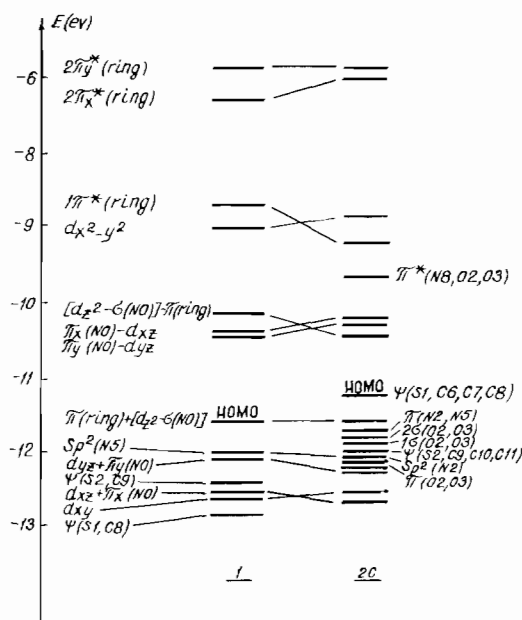


Fig. 6. The diagram of the highest occupied (HOMO) and the lowest unoccupied (LUMO) MOs of **1 (2c)**. Only electron occupancies of the highest occupied MOs are shown.

and nature, are indicated. It follows from Fig. 6 that the molecular orbital diagrams of **1 (2c)** are very typical for iron mononitrosyl complexes with the total number n of d-type electrons on the metal and π electrons of nitric oxide equal to 6 [18, 19]. Indeed, the bonding orbitals $d_{\pi} + \pi(\text{NO})$ and practically non-bonding d_{xy} appeared to be filled while the antibonding orbitals $[d_{z^2} - \sigma(\text{NO})] - \pi(\text{ring})$, $\pi(\text{NO}) - d_{\pi}$ and $d_{x^2 - y^2}$ are empty. At the same time it was shown [18] that the reason for the FeNO group deviation from linearity is pseudo Jahn–Teller mixing of the $\pi(\text{NO}) - d_{\pi}$ and $d_{z^2} - \sigma(\text{NO})$ orbitals, one of which must be populated. As far as both these orbitals are empty in **1 (2c)** a linear geometry of NO coordination should be expected, and in fact is observed (small deviations from linearity $\approx 2\text{--}5^\circ$ can be attributed to intermolecular interactions in crystal packing). The out-of-plane position of the metal ion is also probably a result of pseudo Jahn–Teller mixing of $d_{z^2} - \sigma(\text{NO})$ and $\pi(\text{ring})$ orbitals. Such a mixing is analogous to that of MOs $a_{2u}(\pi)$ and d_{z^2} in iron porphyrin when the displacement of the metal ion from the porphyrin ring plane takes place [18]. It should be noted that the molecular orbital diagrams of both basal ligands are very close to those of the porphyrin ring [18]. Thus, $\pi(\text{ring})$ MO is analogous to $a_{2u}(\pi)$ porphyrin orbital, $1\pi^*(\text{ring})$ to $b_{2u}(\pi^*)$, $2\pi_x^*(\text{ring})$ and $2\pi_y^*(\text{ring})$ to $e_g(\pi^*)$ components, split due to the lower symmetry of both complexes. On this basis one can suggest that the reason for the broad intense shoulder occurring in the visible spectra of **1 (2c)** within the range 350–380

nm is considered to be the transition from $\pi(\text{ring}) + [d_{z^2} - \sigma(\text{NO})]$ MO to $2\pi_x^*$ and $2\pi_y^*$ MOs.

The significant difference in the ligand structures of **1** (**2c**) from porphyrin is in the presence of deprotonated nitrogen atoms (N2 in **1** and N2, N5 in **2c**). The energies of the corresponding lone pairs of electrons $sp^2(\text{N2})$ and $sp^2(\text{N5})$ drastically increase and these orbitals occur in the valence region of the complexes. For this reason the $\pi(\text{N2, N5})$ MO also is present in the valence region of **2c**.

The different nature of the quadridentate ligands in **1** and **2c** leads undoubtedly to a difference in their electronic structures. First, substitution of the H atom at C3 by NO_2 group gives rise to a series of MOs with the main contribution of the oxygen atoms of this group among HOMOs of **2c**. Secondly, substitution of the methyl groups linked to the sulfur atoms by propyl essentially increases (≈ 1 eV), as could be expected, energies of $\Psi(\text{S1, C6, C7, C8})$ and $\Psi(\text{S2, C9, C10, C11})$ MOs in **2c** when compared with $\Psi(\text{S1, C8})$ and $\Psi(\text{S2, C9})$ MOs in **1**.

A considerable energy gap between the LUMO and HOMO (≈ 1 eV $\gg kT$) in the natural way accounts for the ΔE_Q values (Table 6) for **1** (**2c**), which are almost independent of temperature.

In Table 7 data of the iron orbitals population for **1** (**2c**) are given. It will be readily seen that, in terms of electron density distribution on the iron atom, these complexes possess axial symmetry ($N_{p_x} = N_{p_y}$; $N_{d_{xz}} = N_{d_{yz}}$). At the same time the asymmetry of electron density distribution (the difference between d_{z^2} and $d_{x^2-y^2}$ orbitals population) for **1** is markedly more than for **2c**. The determination of the electron density distribution on the iron atom permits one to estimate the relationship between the values of the quadrupole splitting ΔE_Q in the Mössbauer spectra of complexes **1** and **2c**. In fact, the value of the quadrupole splitting (ΔE_Q) is directly proportional to the gradient of the electric field q in the region of the Mössbauer nucleus, which is related to the electronic populations N_i of the i th orbitals of the iron atom by the relationship [20]

$$q = q_d + q_p = \langle r^{-3} \rangle \{ 4/7 [N_{x^2-y^2} - N_{z^2} + N_{xy} - 1/2(N_{xz} + N_{yz})] + 4/5 [1/2(N_x + N_y) - N_z] \} \quad (1)$$

TABLE 7. Populations of the iron orbitals for complexes **1** and **2c**

Complex	p_x	p_y	p_z	$d_{x^2-y^2}$	d_{z^2}	d_{xy}	d_{xz}	d_{yz}
1	0	0	0.19	1.08	1.20	1.97	1.45	1.45
2c	0	0	0.19	1.10	1.17	1.97	1.45	1.46

By substituting the values N_i presented in Table 7 into eqn. (1) the relationship of ΔE_Q for the involved complexes

$$\Delta E_Q(\mathbf{2c})/\Delta E_Q(\mathbf{1}) \approx 1.3 \quad (2)$$

is obtained, which is close to the experimental value (~ 1.4).

The problem of the state of NO in mononitrosyl complexes is of special interest. Our calculations have shown that the orbitals 4σ , 5σ and 2π of nitric oxide are involved in the bonding with the iron atom. In this case the transfer of 0.07 (0.06) and 0.23 (0.24) electrons, respectively, takes place from the 4σ and 5σ orbitals to the iron atom and 0.41 (0.43) electron from the Fe atom to 2π MO of NO for **1** (**2c**), leading to very little net electron transfer. The orbitals 4σ and 2π are antibonding, while 5σ is a bonding orbital. Hence, both the loss of the electron density from the 5σ orbital and its transfer to 2π MO increase the interatomic distance and decrease the force constant in relation to the neutral NO, whereas the decreasing of the 4σ MO population reduces these changes somewhat. As a result the interatomic N–O distance increases a little in **1** (**2c**) when comparing it with the neutral NO from 1.151 [21] to 1.158 (1.167) Å, while the frequency $\nu(\text{NO})$ decreases from 1904 to 1800 (1808) cm^{-1} .

Figure 6 suggests that the reduction of **1** (**2c**) by one electron should lead to population of the $\pi^*(\text{NO})-d_{\pi}$ orbital, that on the one hand will cause the distortion of the FeNO group, and increase the interatomic N–O distance and reduce the value for $\nu(\text{NO})$ on the other hand. Such an experiment will be carried out in the future.

Conclusions

In summary, it should be noted that the electronic structure of the quadridentate ligands is close to that of macrocyclic compounds, in particular, metalloporphyrins, i.e. there is much π -electron delocalization in the concerned ligands. In addition, the results of X-ray analysis, IR, Mössbauer spectra studies and the electronic structure calculations demonstrate that the FeNO moiety in **1** (**2c**) is a highly covalent entity. Within the framework of valence schemes description the FeNO fragment corresponds to the state

$\text{Fe(IV)NO}^- \rightleftharpoons \text{Fe(III)NO}$ significantly displaced to the right. It is necessary to conclude that the geometry of NO coordination on the one hand and the interatomic distance in it and $\nu(\text{NO})$ on the other hand are determined, first of all, not by the realization of one or another valence schemes, but by the total number n of the d-electrons of the metal ion and π -electrons of NO. Thus at $n < 6$ linear NO coordination and values of interatomic distance and $\nu(\text{NO})$ close to the neutral molecule should be expected, whereas at $n > 6$ bent coordination of NO, interatomic distances and $\nu(\text{NO})$ displaced out of the range to the values specific to NO^- should be expected.

Supplementary material

For compounds **1** and **2c** tables of anisotropic temperature factors for all non-hydrogen atoms, hydrogen coordinates and temperature factors (6 pages), and listings of observed and calculated structure factors (13 pages) are available from the authors on request.

References

- 1 K. Ruckpaul and H. Rein, *Cytochrome P-450*, Academic Verlag, Berlin, 1984.
- 2 L. J. Young and L. M. Siegel, *Biochemistry*, **27** (1988) 2790.
- 3 J. C. Fanning, *Coord. Chem. Rev.*, **110** (1991) 235.
- 4 B. B. Wayland and L. W. Olson, *J. Am. Chem. Soc.*, **96** (1974) 6037.
- 5 K. D. Hodges, R. G. Wollmann, S. L. Kessel, D. N. Hendrickson, D. G. Van Derveer and E. K. Barefield, *J. Am. Chem. Soc.*, **101** (1979) 906.
- 6 J. H. Enemark, R. D. Feltham, B. T. Huie, P. L. Johnson and K. B. Swede, *J. Am. Chem. Soc.*, **99** (1977) 3285.
- 7 K. D. Karlin, H. N. Rabinowitz, D. L. Lewis and S. J. Lipard, *Inorg. Chem.*, **16** (1977) 3262.
- 8 N. V. Gerbeleu and V. B. Arion, *Templatnyi Sintez Makrotsiklicheskikh Soedinenii*, Shtiintsa, Kishinev, USSR, 1990.
- 9 S. G. Shova, Yu. A. Simonov, V. B. Arion, M. D. Revenko and T. I. Malinovskii, *Dokl. Akad. Nauk SSSR*, **282** (1985) 1142.
- 10 R. G. Charles, *Org. Synth. Coll.*, **39** (1959) 61.
- 11 B. A. Kazanskii (ed.), *Sintez i Organicheskikh Preparatov*, Izdatel'stvo inostrannoi literaturi, Moscow, 1953, Ch. 4, p. 345.
- 12 N. V. Gerbeleu, V. A. Kogan, V. B. Arion, V. V. Lukov and K. M. Indrichan, *Russ. J. Inorg. Chem.*, **34** (1989) 107.
- 13 G. M. Sheldrick, in G. M. Sheldrick, C. Kruger and R. Goddard (eds.), *Crystallographic Computing 3*, Oxford University Press, London, 1985, pp. 175–189.
- 14 J. A. Ibers and W. C. Hamilton (eds.), *The International Tables for X-Ray Crystallography*, Vol. IV, Kynoch, Birmingham, UK, 1974, Tables 2.2B and 2.3.1.
- 15 Yu. A. Simonov, V. K. Bel'skii, N. V. Gerbeleu, S. G. Shova and V. B. Arion, *Dokl. Akad. Nauk SSSR*, **282** (1985) 620.
- 16 L. M. Epstein, *J. Chem. Phys.*, **36** (1962) 2731.
- 17 Yu. M. Chiumakov, A. S. Dimoglo and I. B. Bersuker, *Zh. Strukt. Khim.*, **14** (1982) 182.
- 18 I. B. Bersuker and S. S. Stavrov, *Coord. Chem. Rev.*, **88** (1988) 1.
- 19 J. H. Enemark and R. D. Feltham, *Coord. Chem. Rev.*, **13** (1974) 339.
- 20 M. Weisbluth, *Hemoglobin. Cooperativity and Electronic Properties*, Chapman and Hall, London, 1974.
- 21 L. Qian, P. Singh, H. Ro and W. E. Hatfield, *Inorg. Chem.*, **29** (1990) 761.